論文 / 著書情報
Article / Book Information

論題(和文)	
Title(English)	Search for EDM of 129Xe using active spin maser
著者(和文)	市川雄一, 佐藤智哉, 大友祐一, 坂本雄, 小島修一郎, 鈴木貴大, 近森正敏, 彦田絵里, 宮武裕和, 七尾翼, 鈴木都文, 土屋真人, 井上壮志, 古川武, 吉見 彰洋, BIDINOSTI Christopher, 猪野 隆, 上野秀樹, 松尾由賀利, 福山武志, 旭耕一郎
Authors(English)	Yuichi Ichikawa, Tomoya Sato, Yuichi Ohtomo, Yu Sakamoto, Shuchirou Kojima, Takahiro Suzuki, Masatoshi Chikamori, Eri Hikota, Hirokazu Miyatake, Tsubasa Nanao, Kunifumi Suzuki, Masato Tsuchiya, Takeshi Inoue, Takeshi Furukawa, Akihiro Yoshimi, Christopher Bidinosti, Takashi Ino, Hideki Ueno, Yukari Matsuo, Takeshi Fukuyama, KOICHIRO ASAHI
出典(和文)	, , , pp. 37-44
Citation(English)	Proceedings of 7th International Workshop on Fundamental Physics Using Atoms (FPUA 2014), , , pp. 37-44
発行日 / Pub. date	2015, 1

Search for EDM in ^{129}Xe using active spin maser

Y. Ichikawa[a,b,*], T. Sato[a], Y. Ohtomo[a], Y. Sakamoto[a], S. Kojima[a], T. Suzuki[a], M. Chikamori[a], E. Hikota[a], H. Miyatake[a], T. Nanao[a], K. Suzuki[a], M. Tsuchiya[a], T. Inoue[c], T. Furukawa[d], A. Yoshimi[e], C. P. Bidinosti[f], T. Ino[g], H. Ueno[b], Y. Matsuo[h], T. Fukuyama[i], K. Asahi[a]

[a]*Department of Physics, Tokyo Institute of Technology, 2-12-1 Oh-okayama, Meguro, Tokyo 152-8551, Japan*
[b]*RIKEN Nishina Center, RIKEN, 2-1 Hirosawa, Wako, Saitama 351-0198, Japan*
[c]*Cyclotron and Radioisotope Center, Tohoku University, 6-3 Aoba, Aramaki, Aoba, Sendai 980-8578, Japan*
[d]*Department of Physics, Tokyo Metropolitan University, 1-1 Minami-Osawa, Hachioji, Tokyo 192-0397, Japan*
[e]*Research Core for Extreme Quantum World, Okayama University, 3-1-1 Tsushimanaka, Kita, Okayama 700-8530, Japan*
[f]*Department of Physics, University of Winnipeg, 515 Portage Avenue, Winnipeg, Manitoba, Canada*
[g]*Institute of Material Structure Science, High Energy Accelerator Research Organization (KEK), 1-1 Oho, Tsukuba, Ibaraki 305-0801, Japan*
[h]*Department of Advanced Sciences, Hosei University, 3-7-2 Kajino-cho, Koganei, Tokyo 184-8584, Japan*
[i]*Research Center for Nuclear Physics (RCNP), Osaka University, 10-1 Mihogaoka, Ibaraki, Osaka 567-0047, Japan*

Abstract

An experimental scheme is under development to search for an electric dipole moment (EDM) in a diamagnetic atom ^{129}Xe through precision measurement of spin precession frequency using a technique of the active nuclear spin maser. A ^{3}He comagnetometer is employed for the magnetometry, in order to cancel out the long-term drifts in the external magnetic field. Also, a double-cell geometry is adopted for a gas cell, which suppresses frequency shifts due to interaction of ^{129}Xe spin with polarized Rb atoms. Recently, the cell design for the double cell has been renewed, and a shield-coil system providing a highly homogeneous magnetic field has been introduced. With improved polarization and longitudinal and transverse spin relaxation times, we have succeeded in operating the dual-species masers of ^{129}Xe and ^{3}He using a double-cell geometry. The EDM measurement on ^{129}Xe aiming at the region of 10^{-28} $e$cm based on the above developments will be started soon.

1. Introduction

The Standard Model of elementary particles is a theory that has passed numerous observational tests of laboratory experiments, and the recent discovery of Higgs particle [1, 2], the last arriving ingredient of the SM, has provided further support for the SM. At the present time, however, most of us cannot avoid dissatisfaction with the SM, since there are numbers of questions unanswered by the SM. For example, the CP violation in the framework of the SM which contributes only to flavor changing processes, as observed in the CP-nonconcerving decays of K and B mesons [3, 4, 5], cannot explain the present matter-dominant Universe [6].

A permanent electric dipole moment (EDM) of a particle, atom, or molecule is the observable directly violating the time reversal symmetry, hence the CP invariance. In particular, the EDM is a flavor diagonal observable, and is sensitive to CP-violating phases beyond the framework of the SM [7]. The size of EDM predicted in the SM is too small to be detected, while most of theories proposed beyond the SM, such as supersymmetry, predict sizes in the regions that are reachable in not very distant future [8]. Thus, the search for EDM constitutes a stringent test which discriminates between the SM and models beyond it. Furthermore, the detection of a finite EDM value should provide a clear evidence for the presence of physics beyond the SM.

The search for EDM is being pursued for various systems [9, 10, 11, 12, 13, 14] with non-zero spin such as neutron, atoms, electron, muon and ions, whose EDMs originate from different CP-violating phases [15]. In a diamagnetic

*Corresponding author
Email address: yuichikawa@riken.jp (Y. Ichikawa)

atom such as ^{129}Xe, the EDM is considered to arise from a CP-odd moment, the Schiff moment S [16], of the nucleus. S is defined as

$$S \equiv \frac{1}{10} \int \rho_{\rm ch}(r) \left(r^2 - \frac{5}{3} \langle r^2 \rangle_{\rm ch} \right) {\rm d}^3 r, \tag{1}$$

where $\rho_{\rm ch}$ represents the charge distribution in the nucleus, and $\langle r^2 \rangle_{\rm ch}$ is the mean square nuclear charge radius. The fundamental CP-violating phases induce CP-odd components in the nucleon-nucleon interactions [17], which then give rise to the Schiff moment. The upper limit of EDM in a diamagnetic atom was obtained for ^{199}Hg as $|d(^{199}{\rm Hg})| < 0.31 \times 10^{-28}$ $e$cm [12]. Since the way by which a nucleus acquires the Schiff moment depends strongly on the nuclear structure, the EDM of diamagnetic atoms should be studied for various nuclear species. The present study aims at measuring the EDM in the diamagnetic atom ^{129}Xe to a size of $|d| = 10^{-28}$ $e$cm, stepping into a domain below the present upper limit, $|d| < 4.1 \times 10^{-27}$ $e$cm [9], by one order of magnitude.

2. Active nuclear spin maser

Experimentally, the value of EDM is determined from difference between the frequencies of ^{129}Xe spin precession measured with the electric field applied parallel and antiparallel to a magnetic field. A search for EDM to a size of $|d| = 10^{-28}$ $e$cm requires the frequency precision at a level of 1 nHz, provided the measurement is done under an electric field of 10 kV/cm.

In the present EDM measurement we employ an active nuclear spin maser [18, 19] which enables us to sustain the spin precession of ^{129}Xe over a long measurement duration. The active spin maser operates in the following manner: In an applied static field B_0 the ^{129}Xe spin is longitudinally polarized through spin exchange with Rb atoms which are optically pumped [20]. Once the ^{129}Xe spin starts precession either by an applied rf field pulse or by a stray noise field, the spin precession is detected optically through Rb atoms which are transversely polarized. By referring to the precession signal thus obtained, a feedback magnetic field $B_{\rm FB}$ rotating in a plane transverse to the B_0 field is generated such that $B_{\rm FB}$ direction is kept orthogonal to the transverse component of spin. When the torque by the $B_{\rm FB}$ is balanced with the rate of the polarization production, the longitudinal spin depolarization and the transverse spin decoherence, the maser oscillation is realized by preventing the decay of the transverse magnetization of ^{129}Xe. Using the spin-maser technique, the frequency precision for the spin precession is expected to be rapidly improved by taking longer and longer observation times for the spin precession.

Notable features of the active spin maser are the optical detection of the spin precession and the artificial production of the feedback field. These features allow us to operate the spin maser with a static magnetic field B_0 as low as ∼mG. On the other hand, in the operation of the conventional type of spin maser [22, 21], magnetic fields of order of ∼G are necessary to run the spin maser because of the need for the feedback field, which is passively generated by the rotating spin magnetization, to be strong enough. The operation of the active spin maser in such a low magnetic field brings in a suppression of frequency uncertainty originating from fluctuation of the magnetic field. A stabilization system for the current in the B_0 solenoid coil was introduced [23]. Large coils surrounding the whole experimental setup were also installed in order to cancel out the environmental magnetic field inside the coil [24]. As a result of these developments, a determination precision of $\delta\nu = 7.9$ nHz for the average frequency in a single-shot measurement of 3×10^4 s was achieved [25].

3. Comagnetometry

3.1. Systematic uncertainties

In an EDM measurement which requires high-precision determination of frequency, the magnetometry is essential in addition to the above improvements on the determination precision of the frequency, because a large systematic uncertainty arises from long-term drifts in frequency. As a matter of fact, the above frequency precision will be meaningful to the EDM detection only if the external magnetic field acting on the ^{129}Xe spins is stable, or its time average is known, to the same level of precision. One of the main causes of the long-term drifts is the drifts in the external magnetic field felt by ^{129}Xe.

A comagnetometer using ^{3}He was incorporated into the nuclear spin maser system in order to cancel out the drift of the external field. ^{3}He is expected to have a negligibly small EDM comparing to ^{129}Xe because of its small

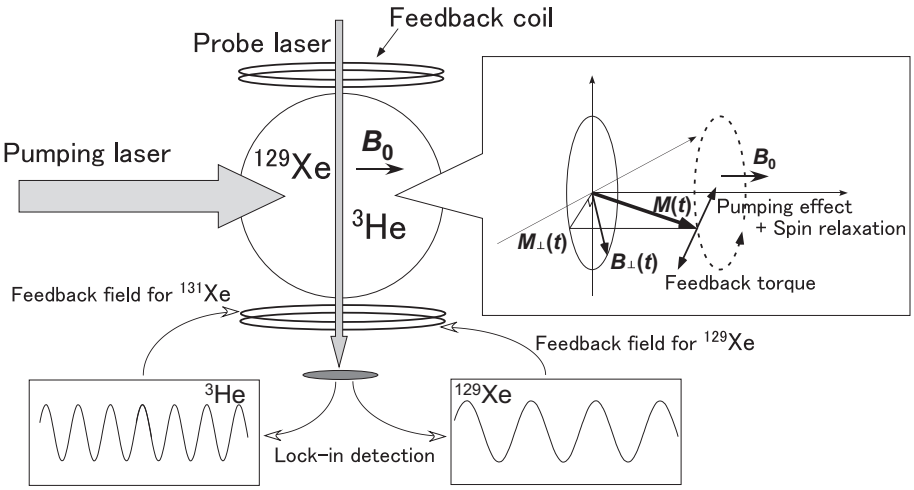

Figure 1: Scheme of active nuclear spin maser of ^{129}Xe equipped with ^{3}He comagnetometer.

atomic number Z. The ^{3}He gas is confined together with ^{129}Xe in a glass cell, so that it directly senses the field that exerts on the ^{129}Xe precession, as an *in situ* magnetometer. The ^{3}He comagnetometer allows us to conduct the EDM measurement as a measurement of difference in the precession phase evolution between ^{129}Xe and ^{3}He, but not the measurement of the individual absolute frequencies which suffer from drifts in the magnetic field.

In addition to the drifts in the external magnetic field, the precession frequency of ^{129}Xe is also affected by drifts in the frequency shift due to the contact interaction of ^{129}Xe spin with polarized Rb valence electrons. The magnitude of the frequency shift is proportional to the polarization P_{Rb} of Rb atoms and the number density [Rb] of Rb vapors. Since the number density [Rb] is strongly dependent of the temperature, the drift in the temperature induces the drifts in the frequency consequently. Unfortunately, the drifts in the frequency shift due to contact interaction with polarized Rb can not be fully removed by the ^{3}He co-magnetometer, because of the different strengths of the Rb-^{129}Xe and Rb-^{3}He contacts [26, 27]. In order to suppress the frequency shift, a double-cell geometry [9] was employed, in which the gas volume is divided into two sections, one for the optical pumping and the other for the masing and the optical spin detection (probing). The double-cell geometry enables us to suppress the Rb polarization in the probe part and thus to reduce the frequency shift.

3.2. Development of ^{3}He comagnetometer

First, the ^{3}He comagnetometer was developed using a glass cell of a spherical shape (single cell). The main difficulty in realizing the ^{3}He comagnetometer stems from the fact that the spin-exchange rate between ^{3}He and Rb is by several orders of magnitude lower than that between ^{129}Xe and Rb. Because there is little source of polarization, spin relaxation at the surface of the cell and impurity in the gas critically degrade the polarization of ^{3}He. Therefore, a GE180 glass with low magnetic impurity and low gas leakage was employed as a material of the cell. The cell is a sphere 20 mm in diameter, containing 1 Torr of ^{129}Xe, 470 Torr of ^{3}He, 100 Torr of buffer N_2 gas, and a trace amount of Rb vapor. The inner surface of the cell is not coated with any agent. We typically achieved 3% of the polarization and over 50 hours of the longitudinal spin relaxation time for ^{3}He at 100 °C.

The gas cell is placed in a box of which the temperature is monitored. The box is placed in a solenoid coil which generates a static magnetic field B_0, and is enclosed in a 4-layer magnetic shield. A circularly polarized pumping laser light parallel to B_0 is incident on the cell. A probe laser light passes through the cell in a direction orthogonal to B_0 and is detected by a photodiode. The signal from the photodiode is divided into two, each being lock-in-amplified with ^{129}Xe or ^{3}He precession frequency, and the resulting two beat signals are obtained and processed individually at the same time to generate their feedback magnetic fields through two separate coils. The scheme of the active nuclear spin maser of ^{129}Xe equipped with the ^{3}He comagnetometer is shown in Fig. 1.

We succeeded in operating the masers of ^{129}Xe and ^{3}He concurrently [28]. The determination precision for the time-average frequency over a 10^6-s period is ∼100 nHz for both the ^{129}Xe and ^{3}He masers.

3.3. Double-cell geometry

In the operation of the active spin maser with the double-cell geometry, there may arise two difficulties, loss of polarization of the ^{129}Xe spins during they diffuse from the pumping part to the probe part, and deterioration of the maser oscillation signal due to the reduced Rb polarization. As for the maser oscillation signal, in the previous work [29], we found that two distinct processes are contributing to the spin detection signal (i.e. the oscillating component in the probe-light transmission intensity measured at the photo diode), for the optical detection, one dependent and the other independent of the Rb polarization. The first process is the repolarization process [19] in which the transverse spin polarization of ^{129}Xe is transferred to Rb atoms via spin exchange and letting the Rb transverse spins follow the ^{129}Xe precession. The second process seemed to come from some presently unidentified origin, and we tentatively regard this phenomenon as follows: The polarization axis for Rb atoms follows adiabatically the instantaneous direction of the magnetic field. Since the field acting on the cell is a vector sum of the applied field B_0 and the dipolar field produced by the polarized ^{129}Xe spins, the Rb polarization is pointed in a direction slightly tilted from B_0 and as a result precesses in synchronization with the ^{129}Xe magnetization. Therefore, the transverse component of Rb polarization is synchronized with the ^{129}Xe precession, thus contributing to the optical spin detection mechanism. The magnitude of such a signal should be proportional to the Rb polarization. This effect should exist in the single-cell geometry, but for the maser with double-cell geometry, this process should tend to be hindered because the Rb polarization is small, and only the repolarization process should be effective.

Bearing the above two difficulties in mind, a double-cell geometry suitable for the dual-species maser operation of ^{129}Xe and ^{3}He was studied. The reduction of ^{129}Xe polarization is a consequence of the summed effects of spin relaxations due to contacts with the inner surfaces of the cell, with Rb vapors and with unpolarized ^{3}He spins during the time in which ^{129}Xe passes through the connection tube of the double cell. If the gas diffusion time is faster than the spin relaxation, the polarization P survives after diffusion to the probe part. The longitudinal spin relaxation time T_1 and the polarization P for ^{129}Xe and ^{3}He were measured by means of adiabatic-fast-passage (AFP) NMR method, for varying tube lengths, surface coating procedures, and partial pressure for ^{129}Xe and ^{3}He.

From the results of the AFP-NMR measurements, the best suited partial pressure of ^{129}Xe is determined to be approximately 1 Torr, in order to eliminate possible ^{3}He spin relaxation due to ^{129}Xe spin and obtain at the same time large enough magnetization of ^{129}Xe. Typically, $T_1 \sim 10$ h and $P \sim 1\%$ for ^{3}He are achieved at a temperature of 80 °C for a GE180 glass cell containing 1 Torr of ^{129}Xe, 425 Torr of ^{3}He and 100 Torr of N_2. The inner surface of the cell was not coated with any agent, because the depolarization of ^{129}Xe is dominated by the contact with unpolarized Rb vapors but not the wall relaxation at temperatures of $80 - 100$ °C. The depolarization of ^{3}He would have been by 10 times or more enhanced by the wall relaxation if the inner surface were coated. By consideration of the measured NMR signal sizes and relaxation of spins during the passage through the connection tube, the tube length was chosen to be less than 15 mm. More details of these developments are described in Ref. [30].

The optical spin detection in the double-cell geometry was tested with a cell with a tube length of 15 mm by observing free induction decay (FID) after the application of an RF pulse. The experimental setup except for the cell was the same as that described in Ref. [28, 29]. We succeeded in observing the FID signal as well as in running the ^{129}Xe maser. On the other hand for ^{3}He, we observed the FID signal but its transverse spin relaxation time T_2 of a few tens of seconds in typical was too short to realize the maser oscillation. The short T_2 is considered to be due to inhomogeneity of the magnetic field in the double-cell volume. Since $T_1 \sim 10$ h for ^{3}He is much longer than the time scale for ^{3}He to travel between the pumping part and the probe part of the double cell, the coherence of ^{3}He spin will be destroyed during the travel in a region with inhomogeneous magnetic field. Therefore the double-cell geometry should be designed by taking into account the homogeneity of the magnetic field over the whole volume of the double cell.

3.4. Renewed experimental setup

In order to improve the homogeneity of the magnetic field, the setup concerning the magnetic environment was renewed. New setup consists of a large triple-layer magnetic shield and a set of solenoid coils to generate the magnetic field B_0.

The large triple-layer shield was designed so that the gaps between the layers were enlarged to 200 mm in order to enhance magnetic flux absorbency. The individual layers of the shield are cylinders of diameter 400 mm, 600 mm and 800 mm, and width 680 mm, 1000 mm and 1300 mm, respectively, from the innermost to outermost layers. The wall

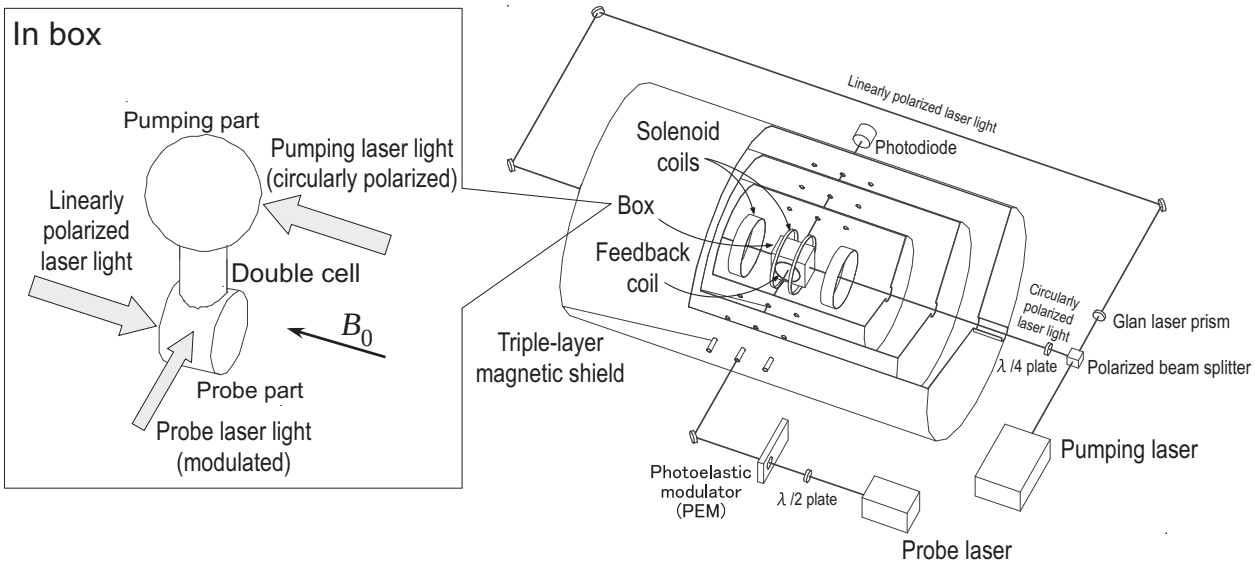

Figure 2: Schematic view of renewed experimental setup. The inset shows the double cell irradiated by laser lights.

thicknesses of the cylinders are all 2 mm. The shield is made of Permalloy with the relative permeability higher than 90,000 and the coercivity higher than 1.0 A/m. Each layer can be closed with end caps, each of which has a 50-mm hole at the center which allows a pumping laser light to enter. Each layer cylinder has 3 holes of 20-mm diameter on both of the left and right sides, so that a probe laser may be inlet from the outside of the shield to the space inside the innermost layer. The innermost layer is equipped with a built-in coil for demagnetization. The residual magnetic field against the earth field was measured to be a few tens of μG which included the magnetization of the shield itself, and thus the shielding factor was over 10^4, which was 10 times better than the previous one used in Refs. [24, 28, 29].

The coil to generate B_0 is located inside the innermost layer of the shield. The coil has a configuration composed of four solenoids with appropriate gaps between them, so that the coil as a whole can avoid blocking the holes on the layers of the magnetic shield. The coil was designed to assure the field homogeneities better than 30 μG/cm and 5 μG/cm for B_0 = 30 mG, in regions within 35 mm and 10 mm from the center, respectively. The detailed design and performance of the coil are described in Ref. [31]. The inhomogeneity in the region within 10 mm from the center was checked from the T_2 measurement for ^{3}He using a single spherical cell with a diameter of 20 mm, where $T_2 = 1.1 \times 10^4$ s was observed, corresponding to the magnetic field gradient of 4.1 μG/cm.

3.5. Dual-species maser operation

Using the above renewed magnetic shield and coil, the experimental setup to obtain the FID signal was reconstructed. The schematic view of the setup is shown in Fig. 2. The double cell is contained in a box of which the temperature is monitored by a thermometer and controlled by heated air blowing. The box is placed in the center of the solenoid coil set which generates a static magnetic field B_0 of approximately 10 mG, and is enclosed in the triple-layer magnetic shield. A circularly polarized pumping laser is incident on the pumping part of the double cell from the B_0 direction. A probe laser light passes through the probe part of the double cell in a direction orthogonal to B_0 and is detected by a photodiode.

New attempt was made in which a linearly polarized laser light was used to irradiate the probe part of the double cell in the B_0 direction. In the previous work [29], the frequency shift was reduced by a factor of 10 or more by employing the double-cell geometry as compared to the single-cell geometry, although the frequency shift remained to exist, which seemed to stem from the longitudinal repolarization of Rb atoms generated by polarized ^{129}Xe and ^{3}He. We therefore introduced the linearly polarized laser light in order to eliminate actively the remaining frequency shift. The capability to detect spins optically in the presence of the linearly polarized laser light was tested for both ^{129}Xe and ^{3}He [29, 32]. In this test, a laser light from a taper-amplified distributed feedback (TA-DFB) laser with a wave length of 794.76 nm and a line width of 10 MHz was divided into two beams, one with a power of 1.0 W

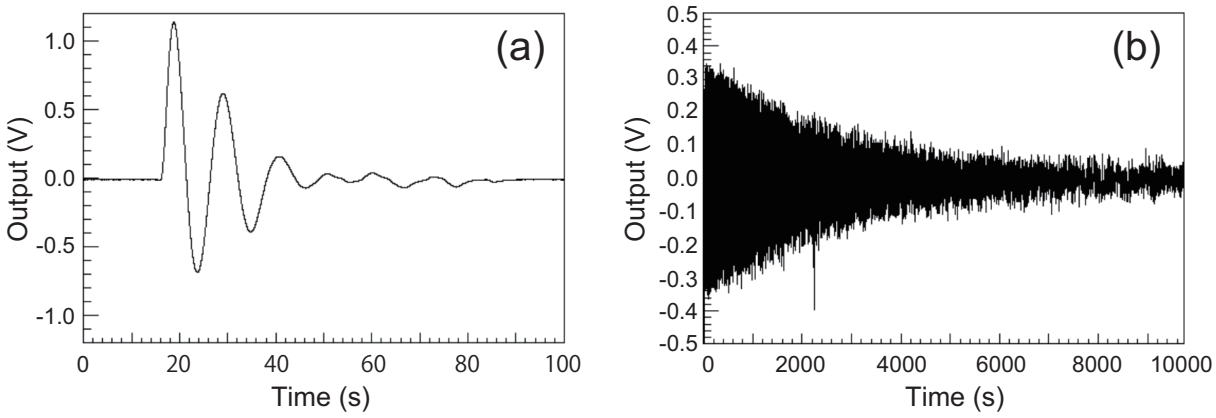

Figure 3: (a) FID signal obtained using a cell with 15-mm tube. (b) FID signal obtained using a cell with 5-mm tube. The temperature was set to approximately 90 °C

irradiating the pumping part of the cell after the production of circular polarization through a $\lambda/4$ plate, and the other with a power of 0.3 W irradiating the probe part of the cell after the production of linear polarization through a Glan laser prism.

The FID signals were obtained for two double cells. The first double cell consisted of a sphere 20 mm in diameter for pumping, and a cylinder 15 mm in diameter, 10-mm thick for probing, connected each other by a 15-mm long tube. The second double cell had the same geometry as the first one had, except that the connecting tube was 5-mm long. Since the coil was designed to implement the homogeneity of 30 muG/cm for B_0 = 30 mG (i.e. 10^{-3}/cm) in the region within 35 mm from the center as mentioned above, the former double cell extended out of the high homogeneity region while the latter one stayed within the region. As a result of the FID measurements, T_2 were determined to be 13 s and 2,340 s for the former and the latter cells, respectively, as shown in Fig. 3 (a) and (b). According to the improved homogeneity throughout the whole volume of the double cell, we have improved T_2 by two orders of magnitude from the previous one.

By virtue of the above improvements in the polarization P and the transverse spin relaxation time T_2 of ^{3}He, the amplitude of the maser oscillation was expected to be enhanced, because the amplitude under the optimized feedback field is given as

$$V_{\mathrm{maser}} \propto P\sqrt{\frac{T_2}{T_1^*}}, \tag{2}$$

where P is the polarization, and T_1^* is the effective spin relaxation time including the pumping effect.

In the operation of the active spin maser with the ^{3}He comagnetometer, the signal from the photodiode is divided into two, each being lock-in-amplified with ^{129}Xe or ^{3}He precession frequency, and the resulting two beat signals are stored in a disk in a computer and at the same time are processed individually to generate their feedback magnetic fields B_{FB} with two separate coils. In this measurement, powers of the pumping laser light and the linearly polarized laser light illuminating the cell were adjusted to be 1.0 W and 0.2 W, respectively. We succeeded in operating the masers of ^{3}He and ^{129}Xe concurrently, as shown in Fig. 4. Details of the dual-species maser operation is described in Ref. [32]. Although the stability of the maser oscillation is not enough in the current situation, it is expected to improve through refined optimization.

4. Towards the EDM measurement

The basic schemes for the precision measurement of spin precession frequency have been established, by incorporating the ^{3}He comagnetometer into the active nuclear spin maser of ^{129}Xe. In the EDM measurement the measurement should be done in the presence of an electric field, where electrodes to apply the electric field are attached on the probe part of the double cell.

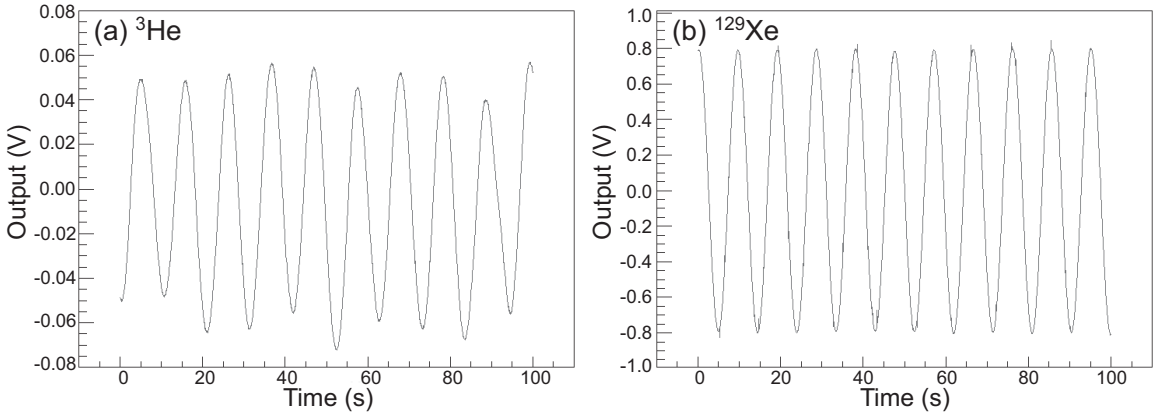

Figure 4: Dual maser oscillation of (a) ^{3}He and (b) ^{129}Xe over a typical time period of 100 s. The beat signals lock-in-amplified for ^{3}He and ^{129}Xe were generated upon the reference frequency of 31.39 Hz and 11.38 Hz, respectively. The temperature is set to approximately 90 °C.

In the previous work [28], we carried out a first trial of the EDM measurement using a double-cell equipped with Mo electrodes, where the maser signal of ^{129}Xe and the FID signal of ^{3}He were observed simultaneously under an electric field of 1.5 kV/cm with a measured leakage current of 620 pA.

In our current experimental scheme, the linearly polarized laser light has to be introduced parallel to B_0, thus through the electrodes. Therefore we consider as candidates of transparent electrodes, ITO electrodes evaporated on plane glasses, and wire-mesh electrodes. Using the ITO electrodes we have successfully applied an electric field up to 7.0 kV/cm with a leakage current of 130 pA.

As described above, the electric field has been successfully applied, without any discharge in some cases. However the optimum condition for the maser oscillation of ^{129}Xe and ^{3}He will vary as the polarization P changes due to the contact with the surface of the electrodes. In both cases of using ITO and wire-mesh electrodes, the change of P and the resulting optimum condition for the maser operation should be studied.

5. Summary and future outlook

In order to search for EDM in the ^{129}Xe atom, which is sensitive to extra CP violation beyond the Standard Model, we have been studying the experimental scheme for the precision measurement of the ^{129}Xe spin precession using the active nuclear spin maser technique. For the magnetometry, a ^{3}He comagnetometer was incorporated to the ^{129}Xe spin maser system. Also, a double-cell geometry was employed in the gas cell in order to suppress the frequency shift due to the contact interaction with polarized Rb atoms. We improved the polarization, the longitudinal spin relaxation time and the transverse spin relaxation time by finding out the cell design suited for the double cell containing both ^{129}Xe and ^{3}He and by renewing the experimental setup so that it provides highly homogeneous magnetic field. As a result, we have succeeded in operating the dual masers of ^{129}Xe and ^{3}He using the double-cell geometry. Incorporation of the ^{3}He comagnetometer into the double cell may bring out its primary potential to cancel out the long-term drift in the frequency. Consequently a dramatic improvement in the frequency precision is expected by taking advantage of the long measurement duration using the active spin maser.

In addition to these developments of the basic schemes for the precision EDM measurement, the performance of a cell equipped with the electrodes should be studied for the EDM measurement. We should also take considerable steps to deal with systematic uncertainties which should become apparent in the present schemes. The performance of the ^{3}He comagnetometer will be checked by taking the correlation between the ^{129}Xe and ^{3}He frequencies. The reduction of the frequency shift due to the polarized Rb, and in particular the condition for the irradiation of the linearly polarized laser light should be sought out. Furthermore, a digital feedback system which is capable of suppressing the uncertainties due to artificial production of the feedback field $B_{\rm FB}$ is being developed [33]. The EDM measurement on ^{129}Xe aiming at the region of 10^{-28} $e$cm based on all the above developments and studies will be started.

Acknowledgments

This work was partly supported by the JSPS KAKENHI (No.21104004 and No.21244029). T. Sato acknowledges the JSPS Research Fellowships for Young Scientist.

References

[1] ATLAS Collaboration, Phys. Lett. B **716**, 1 (2012).
[2] CMS Collaboration, Phys. Lett. B **716**, 30 (2012).
[3] J. H. Christenson *et al.*, Phys. Rev. Lett. **13**, 138 (1964).
[4] B. Aubert *et al.*, Phys. Rev. Lett. **87**, 091801 (2001).
[5] K. Abe *et al.*, Phys. Rev. Lett. **87**, 091802 (2001).
[6] A. D. M. Sakharov, Sov. Phys. JETP Lett. **5**, 24 (1967).
[7] I. B. Khriplovich and S. K. Lamoreaux, CP Violation Without Strangeness (Springer, New York, 1997).
[8] M. Pospelov and A. Ritz, Ann. Phys. **318**, 119 (2005).
[9] M. A. Rosenberry *et al.*, Phys. Rev. Lett. **86**, 22 (2001).
[10] B. Regan *et al.*, Phys. Rev. Lett. **88**, 071805 (2002).
[11] C. A. Baker *et al.*, Phys. Rev. Lett. **97**, 131801 (2006).
[12] W. C. Griffith *et al.*, Phys. Rev. Lett. **102**, 101601 (2009).
[13] J. J. Hudson *et al.*, Nature **472**, 493 (2011).
[14] The ACME Collaboration, Science **343**, 269 (2014).
[15] J. S. M. Ginges and V. V. Flambaum, Phys. Rep. **397**, 63 (2004).
[16] L. I. Schiff *et al.*, Phys. Rev. **132**, 2194 (1963).
[17] J. Hisano, Y. Shimizu, Phys. Rev. D **70**, 093001 (2004).
[18] A. Yoshimi *et al.*, Phys. Lett. A **304**, 13 (2002) .
[19] A. Yoshimi *et al.*, Phys. Lett. A **376**, 1924 (2012) .
[20] W. Happer *et al.*, Rev. Mod. Phys. **44**, 169 (1972).
[21] T. E. Chupp *et al.*, Phys. Rev. Lett. **77**, 3971 (1994).
[22] M. G. Richards *et al.*, J. Phys. B **21**, 665 (1988).
[23] T. Furukawa *et al.*, J. Phys.: Conf. Ser. **312**, 102005 (2011).
[24] T. Inoue *et al.*, Physica E **43**, 847 (2011).
[25] T. Inoue *et al.*, to be published.
[26] Z. L. Ma *et al.*, Phys. Rev. Lett. **106**, 193005 (2011).
[27] M. V. Romalis *et al.*, Phys. Rev. A **58**, 3004 (1998).
[28] Y. Ichikawa *et al.*, Eur. Phys. J.: Web of Conf. **66**, 05007 (2014).
[29] E. Hikota *et al.*, Eur. Phys. J.: Web of Conf. **66**, 05005 (2014).
[30] Y. Ohtomo *et al.*, Proceedings of FPUA2014 (this proceedings).
[31] Y. Sakamoto *et al.*, Proceedings of FPUA2014 (this proceedings).
[32] T. Sato *et al.*, Proceedings of FPUA2014 (this proceedings).
[33] S. Kojima *et al.*, Proceedings of FPUA2014 (this proceedings).